Modeling the *In Vivo* Corrosion of Magnesium Alloys:
A Biodegradable Alternative to Traditional Orthopedic Implants

BEE 4530: Computer-Aided Engineering, Applications to Biomedical Processes
Anna Botto
Nina Jain
Haadea Khan
Liza Man

Contents

1.0 Executive Summary

Magnesium offers a promising alternative to traditional orthopedic implant materials, as it is both biodegradable and osteoconductive. Like traditional implants, magnesium has the mechanical properties necessary to support the surrounding tissue as it heals. Magnesium corrodes when placed into the body, and its osteoconductive properties allow it to be replaced by native bone, eliminating the need for further surgery.

The main concern is that pure magnesium implants have been found to degrade too rapidly when studied *in vitro*. This may lead to catastrophic loss of mechanical integrity as well as potentially lethal production of magnesium ions, hydroxide ions, magnesium hydroxide, and hydrogen gas—all byproducts of the corrosion process. No animal studies using pure magnesium implants have been conducted. However, the magnesium alloy, LAE442, which as been studied in animal models, has been shown to have a slower corrosion rate when compared to pure magnesium *in vitro* models.

Our goal for this study was twofold; we aimed to 1) determine the time required for complete corrosion of both materials after implantation and 2) monitor the concentrations of magnesium ions, hydroxide ions, and magnesium hydroxide as they were affected by the corrosion of both the pure magnesium and LAE442 implants. We developed a two-dimensional axisymmetric model of a rod implanted into the medullary cavity of a human femur using COMSOL Multiphysics 4.3b. Our computational domain consisted of the bone tissue that surrounded the implant. As the implant degraded over time, the boundary between the bone and the implant moved inward toward the axis of symmetry. There was also a corresponding flux of magnesium ions across this boundary, allowing us to model the diffusion and reaction of magnesium ions, hydroxide ions, and magnesium hydroxide in the bone. The main difference between the model of the pure magnesium and that of the LAE442 implant was that the velocity of the moving boundary and the flux of magnesium ions across the implant-bone interface were smaller in the latter model.

Since the corrosion rate of the pure magnesium implant was faster than that of the LAE442 alloy, the pure magnesium implant completely degraded in 182 days, compared to 1570 days for the alloy. Due to this faster corrosion rate, there was a greater build-up of magnesium ions and magnesium hydroxide in the pure magnesium model than from the LAE442 alloy after 28 days. For both of these species, the highest concentrations occurred at the point where the line of planar symmetry intersected with the implant-bone interface. The hydroxide ion concentration, however, was lower in the pure magnesium model since the greater build up of magnesium ions lead to a faster consumption of hydroxide ions. The highest hydroxide ion concentration in both models was found at the outer edge of the femur, furthest from the implant.

While our model indicated that the decrease in hydroxide concentration was small enough to prevent formation of a toxic acidic environment, our results also indicated that both implants resulted in intolerable concentrations of hydrogen gas. Therefore, neither the pure magnesium nor the LAE442 alloy implants are safe for use in human patients. Further work to develop a slower corroding magnesium alloy is necessary.

2.0 Introduction

2.1 Background

The treatment of bone fractures commonly involves the use of internal fixation devices such as screws, pins, plates, and rods [1]. These internal fixation devices aid in the fracture-healing process by stabilizing the fracture in anatomical alignment and by providing mechanical support. Since these devices are traditionally stainless steel-based or titanium-based alloys, they do not degrade in the body and must be removed during a second surgery [2]. The requirement for a second surgery dramatically increases the cost of treatment as well as the risk of medical complications. Traditional fixation materials are also known to cause chronic inflammatory responses that may lead to irritation, discomfort, and failure of the implant [3].

Magnesium orthopedic implants offer a promising alternative to traditional stainless steel and titanium-based devices. The mechanical properties of magnesium implants are more similar to those of bone than are the properties of currently employed materials [4]. In addition, the bone is the body's largest magnesium reservoir [5]. Magnesium implants also promote the growth of osteoblasts; they have been found to be *osteoconductive* in both *in vitro* and *in vivo* experiments [4,6]. Since magnesium implants are readily corroded when placed in a physiological environment, they can be designed in a way that allows complete bone regrowth and implant corrosion—eliminating the need for a second surgery.

A major hurdle to the use of pure magnesium implants *in vivo* is that they may degrade too rapidly before the native tissue has had time to regrow and regain its mechanical strength [6]. This rapid degradation not only causes catastrophic loss of mechanical integrity, but also leads to the formation of magnesium ions (Mg^{2+}), hydroxide ions (OH^-), magnesium hydroxide ($Mg(OH)_2$), and hydrogen gas (H_2). The concentrations of these species may accumulate to toxic levels [2].

Various magnesium alloys, however, have been proposed as a solution to this problem. In particular, the addition of certain metals, especially rare earth elements, to pure magnesium implants can significantly slow down the corrosion process [6]. The magnesium alloy, LAE442, which contains 90 weight percent magnesium, 4 weight percent lithium, 4 weight percent aluminum, and 2 weight percent rare earth elements, is a promising alternative. Although Witte et al. have thoroughly investigated the corrosive properties of LAE442 in animal models, they have not tested these alloy implants in humans.

In our study, we modeled the corrosion of both pure magnesium and LAE442 when implanted as a rod into the center of the human femur. The corrosion rate of pure magnesium was taken from *in vitro* data; the corrosion rate and flux of magnesium ions were pH dependent. These same values for the alloy were taken from *in vivo* studies and were not pH dependent. From this data, we modeled the concentration of magnesium ions, hydroxide ions, and magnesium hydroxide in the bone surrounding the implant, taking into account both the diffusion and reaction of these three species. It was not necessary to model the volume of hydrogen gas evolved, as it did not participate in the reaction modeled, and the amount produced was directly proportional to the mass of magnesium ions [7].

2.2 Design Objectives

The specific design objectives were as follows:

1) Determine the time required for complete corrosion of the pure magnesium rod in the human femur and compare this to the corrosion rate of the LAE442 as determined by *in vivo* studies.
2) Monitor magnesium ion, hydroxide ion, and magnesium hydroxide concentrations in the femur for 28 days and compare these levels with the maximum tolerable concentrations in the human body to assess toxicity of the two implant materials.

3.0 Problem Formulation

3.1 Model Design and Schematic

Figure 1 a shows an x-ray image of a rod implanted into the femur [8]. This is the geometry that we modeled. Both the pure magnesium and LAE442 alloy implants corroded over time. The pattern of their corrosion is shown in Figure 1 b [9]. This figure tracked the corrosion of a magnesium pin implanted into a rat femur over the course of 24 weeks. The implant remained cylindrical for the first four weeks of this study, which is the time period we investigated in our model.
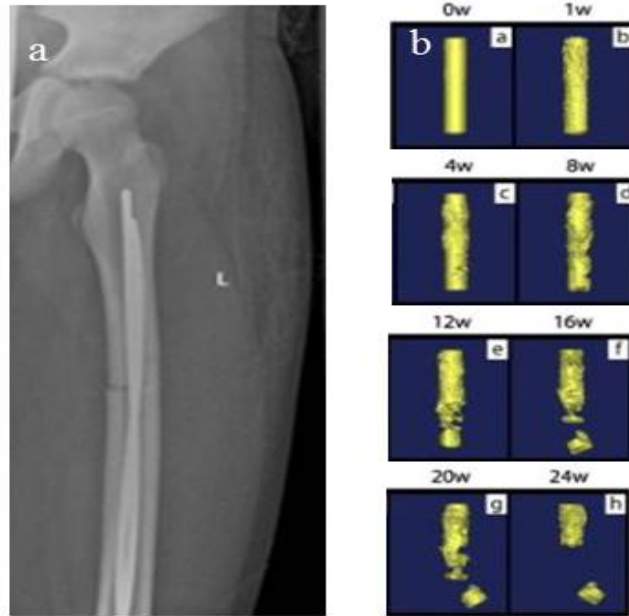

Figure 1. *(a) X-ray image of rod implanted into human femur. (b) 3D reconstruction of magnesium rod degrading in rate femur [8,9].*

We simplified the geometry of the implant and femur to be perfect cylinders. Although this was not a very realistic approximation at the top and bottom of the femur, it was a relatively good approximation throughout the middle of the femur where the rod was implanted. The femur was modeled as a two dimensional axisymmetric domain. Our computational domain included

the bone tissue surrounding the implant but not the implant itself. We further simplified our domain by cutting it along the line of planar symmetry (Figure 2).
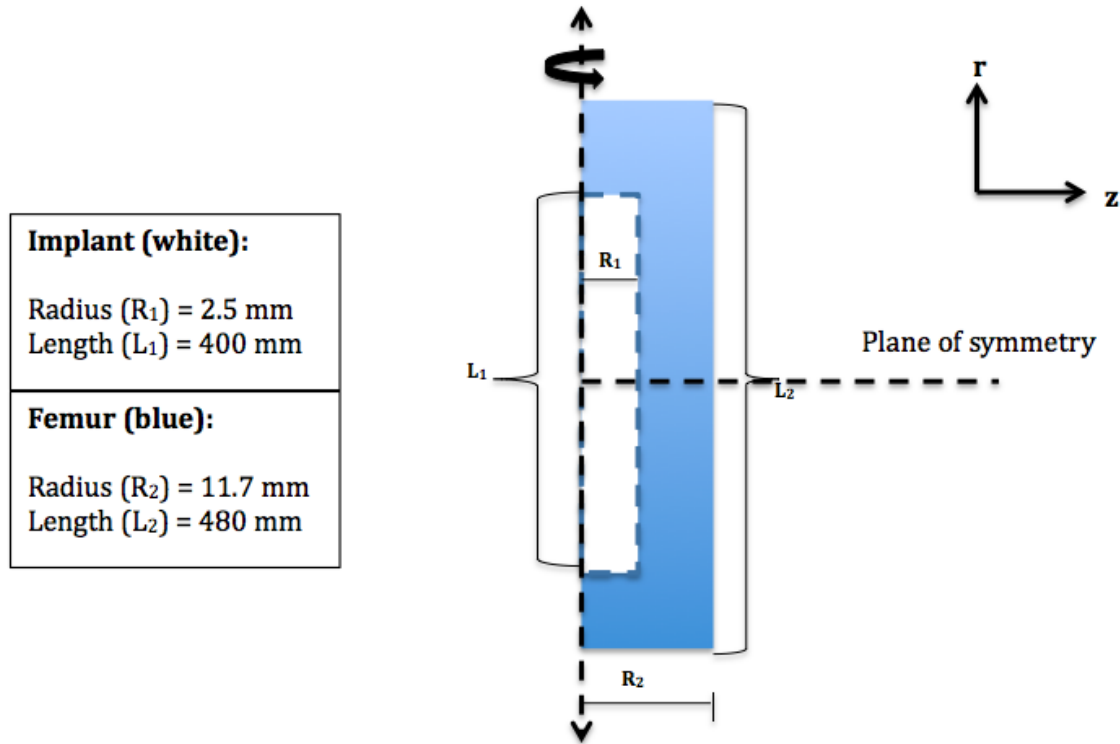

Figure 2. Schematic of computational domain. The blue represented the femur bone tissue surrounding the implant. The implant (white) was not part of the domain. We used a two dimensional axisymmetric domain to model the femur.

The length, 480 mm, and radius, 11.7 mm, of the femur were taken to be the average length and radius of a human femur [10]. The radius of the implant, 2.5 mm, was taken to be one of the standard implant sizes available, while the length, 400 mm, was chosen so that the implant was only as long as the central cylindrical portion of the femur. This allowed us to use a two dimensional axisymmetric domain. For further discussion of the boundary conditions and governing equations used, (Appendix A).

4.0 Results and Discussion

4.1 Solution

The corrosion rates of the two implant materials studied, pure magnesium (Figure 3 a, b, c, and d) and LAE442 (Figure 3 e, f, g and h) were compared. Since the corrosion rate of the pure magnesium implant was pH-dependent, it was updated at each time step. Therefore, the time required for complete corrosion of the implant was an output of the pure magnesium model. For the LAE442 alloy, the corrosion rate was taken from *in vivo* data. Thus, it was not necessary to implement pH dependence, for the corrosion rate was simply specified as an input parameter. See Appendix A for further discussion of model implementation.
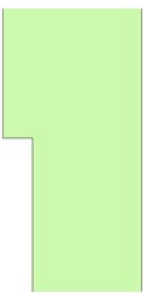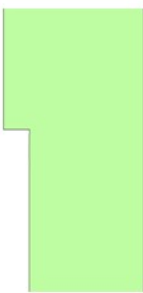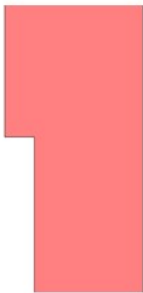
	0 Days	28 Days	182 Days	1570 Days
Pure Magnesium Implant	a	b	c	d
LAE442 Alloy Implant	e	f	g	h

Figure 3. Corrosion of pure magnesium and LAE442 alloy over time. The pure magnesium implant degraded completely after 182 days or 6.5 months while the alloy took 1570 days or 4.3 years to corrode completely.

The pure magnesium implant corroded more rapidly than did the LAE442 alloy; the pure magnesium rod corroded completely in 182 days while the LAE442 alloy took 1570 days (Figure 3). These values corresponded to average corrosion rates of 5.017 mm/year and 0.58 mm/year for the pure magnesium and LAE442 implants, respectively. The faster corrosion rate of pure magnesium resulted in higher concentrations in the bone of both magnesium ions and magnesium hydroxide when compared to the LAE442 alloy at the same time step. This can be seen in the comparison of the concentrations of all three species, magnesium ions, hydroxide ions, and magnesium hydroxide at 28 days as a result of pure magnesium and LAE442 corrosion (Figure 4).

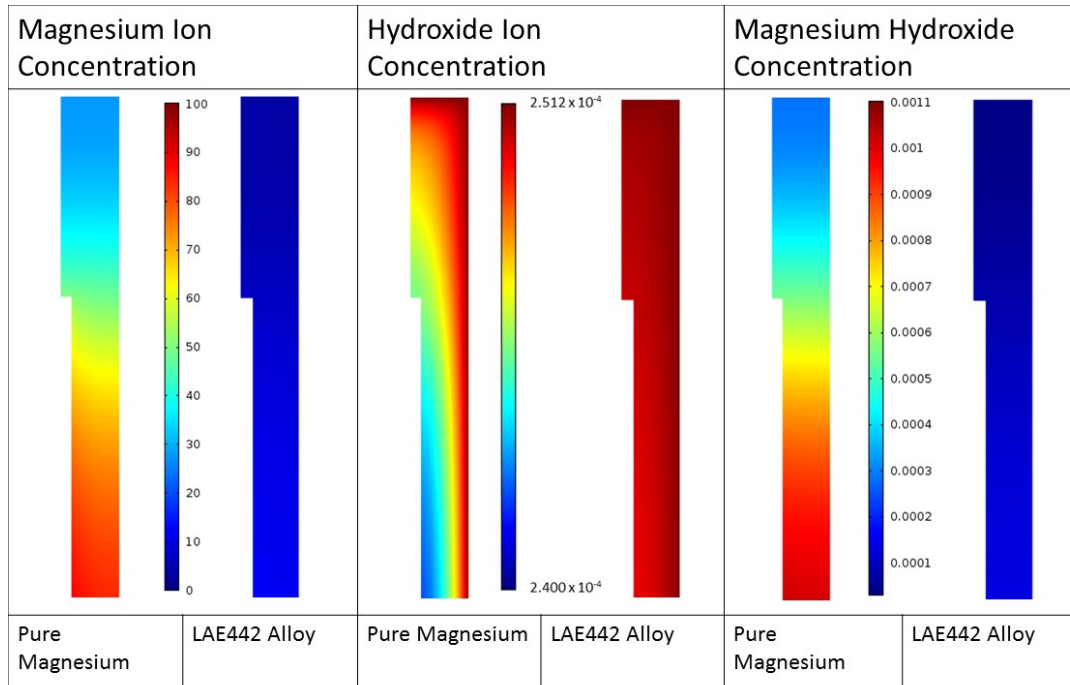| Magnesium Ion Concentration	Hydroxide Ion Concentration	Magnesium Hydroxide Concentration
Pure Magnesium / LAE442 Alloy	Pure Magnesium / LAE442 Alloy	Pure Magnesium / LAE442 Alloy

Figure 4. Concentration profiles in the bone after 28 days in the top 100 mm of geometry.

The concentrations of magnesium ions and magnesium hydroxide were higher in the femur implanted with pure magnesium than in that implanted with LAE442 alloy (Figure 4). This was due to the higher corrosion rate of the pure magnesium implant. The hydroxide ion concentration, however, was higher in the case of the LAE442 alloy. In our model, hydroxide ions were consumed when they reacted with magnesium ions. Because there were fewer magnesium ions in the femur implanted with LAE442, fewer hydroxide ions were consumed. For both the pure magnesium and LAE442 implants, the concentrations of magnesium ions and magnesium hydroxide were highest at the point where the line of planar symmetry intersected the implant-bone interface. The hydroxide ion concentrations, however, were highest in the upper right corner of the femur. This was due to the constant concentration boundary condition applied along the outer edge of the femur ($C_{OH} = 2.512*10^{-4}$ mol/m^3).

To better study the change in concentration with time, plots of magnesium ion, hydroxide ion, and magnesium hydroxide concentrations at the point (r = 2.5 mm, z = 240 mm) as a function of time were generated. This is the point mentioned above where the line of planar symmetry intersected the implant-bone interface. These plots are shown in Figures 5, 6, and 7.

Figure 5. *Magnesium ion concentration at the point (r = 2.5 mm, z = 240mm) as a function of time for both the pure magnesium and LAE442 alloy implants. Inset image shows location of point used for analysis.*

The magnesium ion concentration increased more rapidly in the femur with the pure magnesium implant than in the femur with the LAE442 alloy implant (Figure 5). Similarly, the hydroxide ion concentration changed more rapidly in the case of the pure magnesium implant than with the LAE442 alloy implant. However, the hydroxide ion concentration *decreased* from its initial value as hydroxide reacted with magnesium ions (Figure 6).

Figure 6. *Hydroxide ion concentration as a function of time at the point (r = 2.5mm, z = 240mm) for both the pure magnesium and LAE442 alloy implants. Inset image shows location of point used for analysis.*

As mentioned previously, the corrosion rate of the pure magnesium implant was pH dependent. As hydroxide ions were consumed, the pH in the femur decreased, the corrosion rate of the implant increased, and more magnesium ions were evolved (Appendix A). This caused the hydroxide ions to be more rapidly consumed. In addition to affecting the corrosion rate, the decrease in hydroxide ions corresponded to an increase in magnesium hydroxide concentration. Magnesium hydroxide was the product of the reaction of magnesium ions with hydroxide ions, and its concentration was plotted over time (Figure 7).
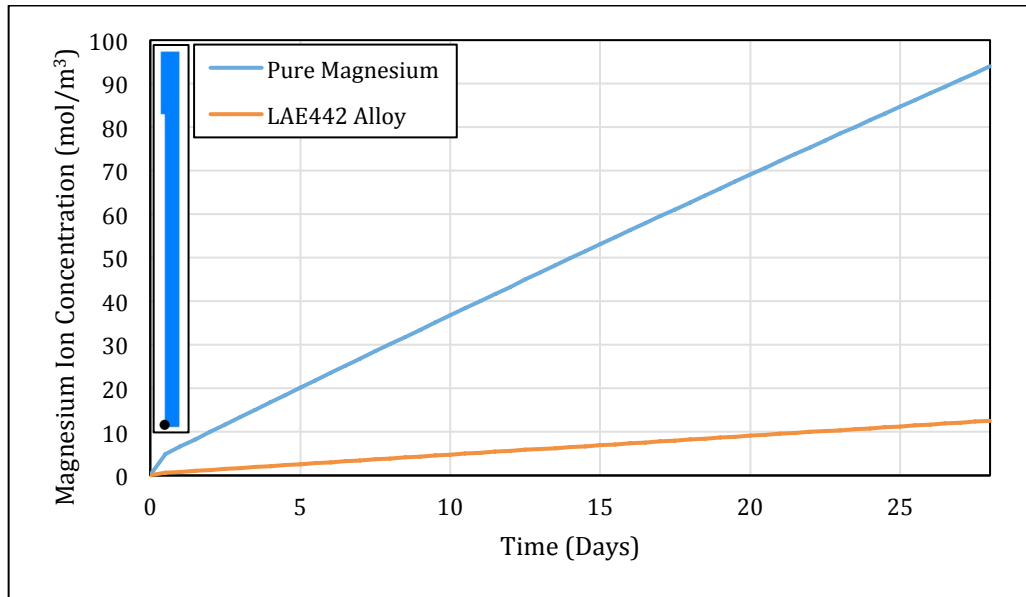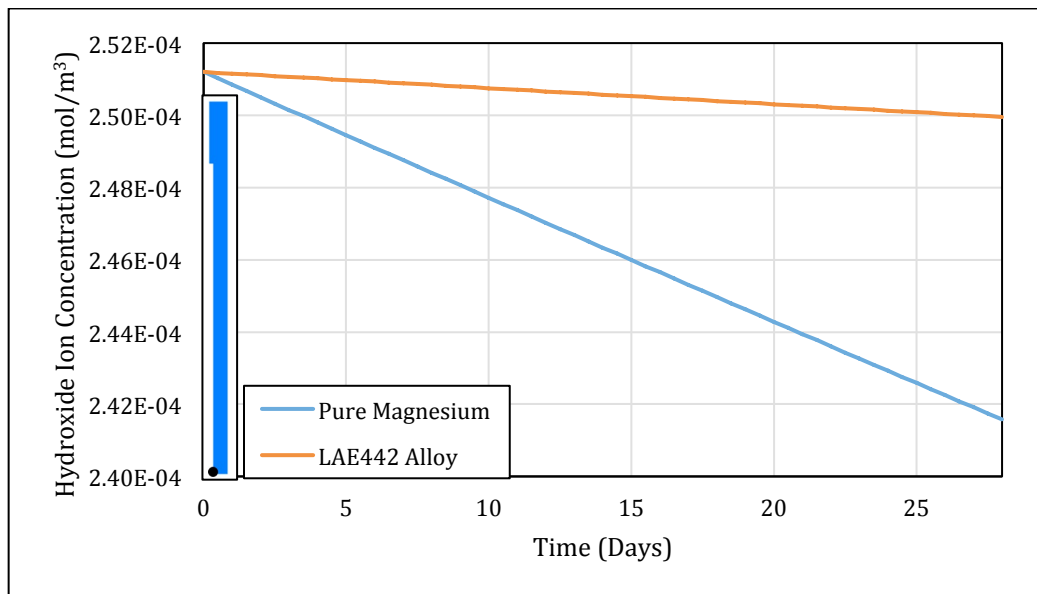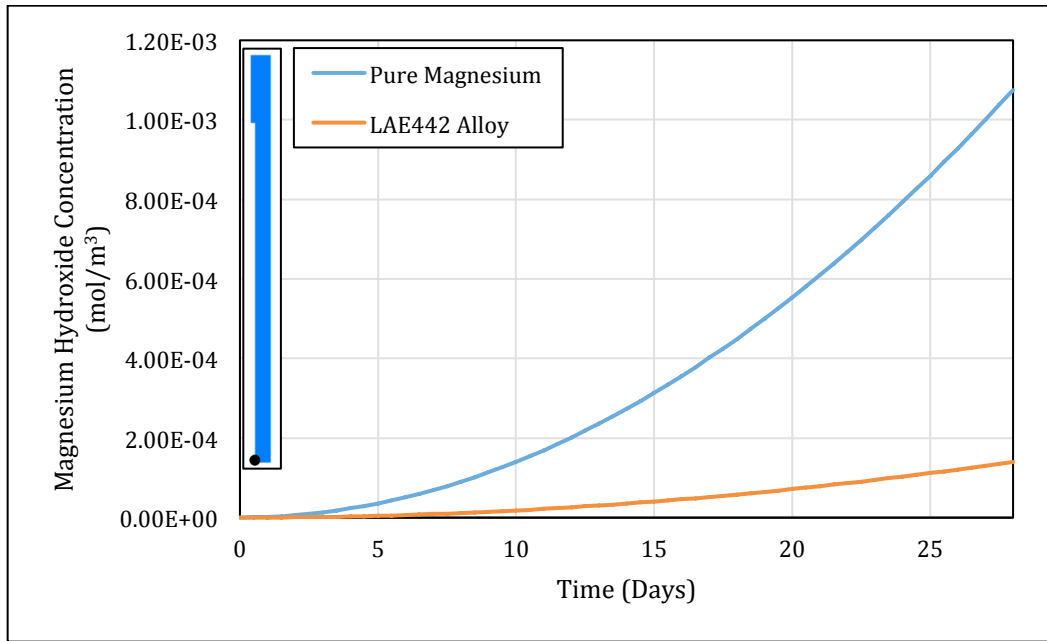

Figure 7. Magnesium hydroxide concentration at the point (r = 2.5 mm, z = 240mm) as a function of time for both the pure magnesium and LAE442 alloy implant. Inset image show location of point used for analysis.

The magnesium hydroxide concentration increased more rapidly in the case of the pure magnesium due to the faster corrosion rate discussed above. Figures 5, 6, and 7 demonstrated the change in concentrations with time. Figures 8, 9, and 10 below further examined the concentration profiles along the line of planar symmetry (Figure 8).

Figure 8. *Magnesium ion concentration as a function of position along the axis of planar symmetry 28 days after implantation. Inset image shows location of line used for analysis.*

The concentration of magnesium ions evolved from the pure magnesium implant was one order of magnitude higher than that produced by the LAE442 alloy implant. Note the logarithmic scale used in Figure 8. The concentration of magnesium ions was highest at the implant-bone interface and decreased toward the outer edge of the femur. As the implant was not part of our domain, concentration values were only calculated for the femur. At the time step used, 28 days, the implant was smaller in the case of the pure implant, for it had degraded more than the LAE442 implant.

The hydroxide ion concentration varied less between the two implants than did the magnesium ion concentration. The hydroxide ion concentration was also plotted along the line of planar symmetry (Figure 9).

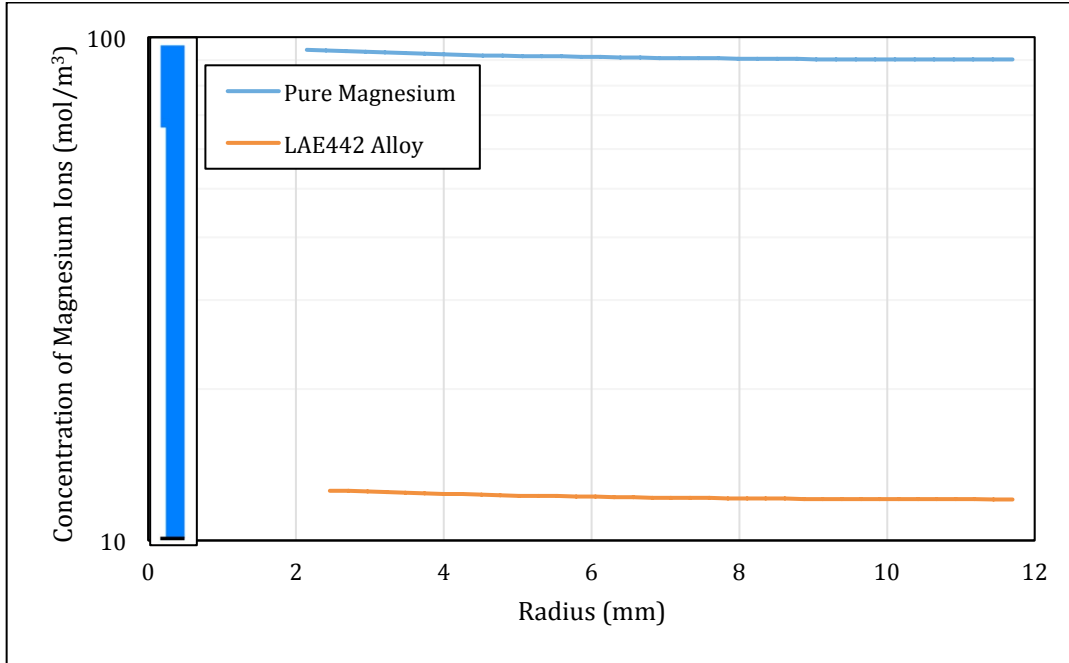***Figure 9***. *Hydroxide ion concentration as a function of position along the axis of planar symmetry days 28 after implantation. Inset image shows location of line used for analysis.*

The concentration of hydroxide ions was highest along the outer edge of the femur and lowest at the implant-bone interface. Hydroxide ion concentration was lower in the femur implanted with pure magnesium. This was due to the higher concentration of magnesium ions evolved from the pure magnesium implant, which allowed more hydroxide ions to react to form magnesium hydroxide. This resulted in a higher concentration of magnesium hydroxide in the case of the pure magnesium implant (Figure 10).

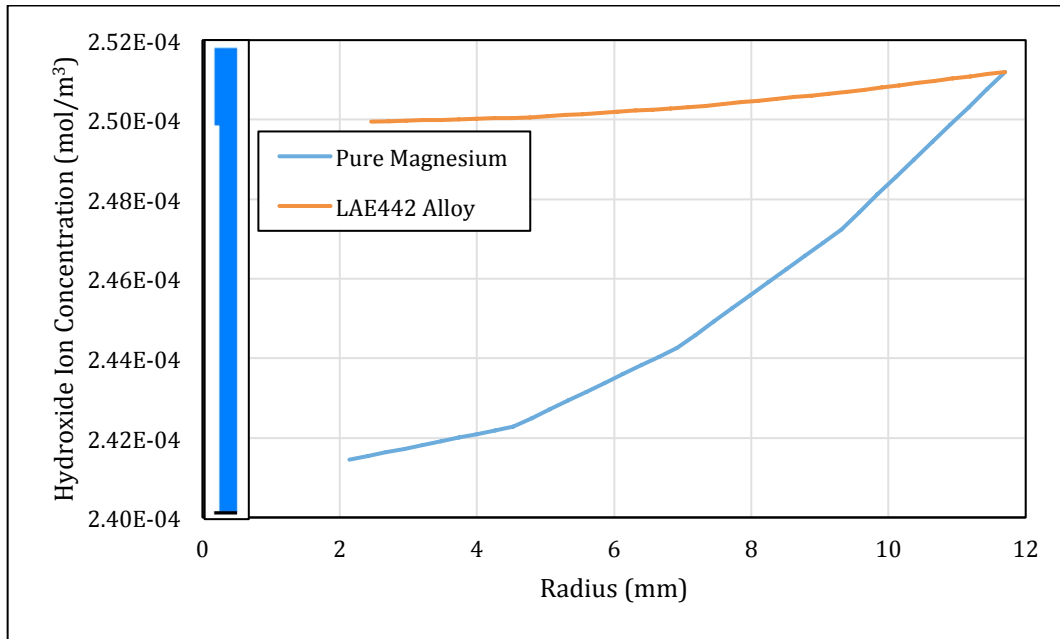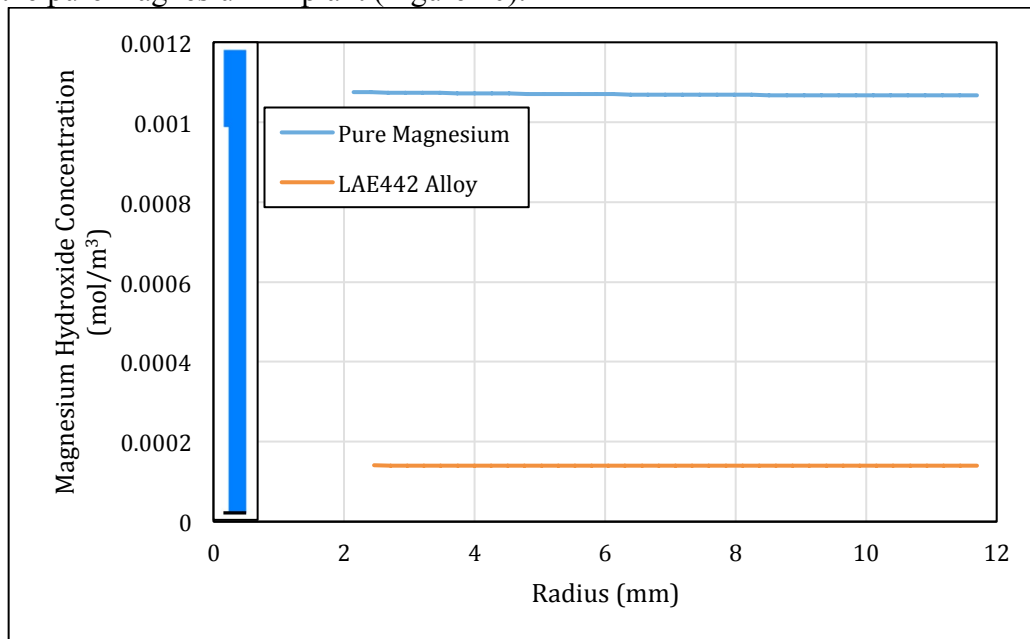***Figure 10***. *Magnesium hydroxide concentration as a function of position along the axis of planar symmetry after 28 days. Inset image shows location of line used for analysis.*

The faster corrosion rate of the pure magnesium implant compared with that of the LAE442 alloy not only caused the implant to degrade in a shorter amount of time, 182 versus 1570 days, but also increased the concentrations of magnesium ions and magnesium hydroxide in the femur after 28 days. For both of these species, the highest concentrations accumulated at the point where the line of planar symmetry intersected the implant-bone interface. The hydroxide ion concentration, however, was lower in the case of pure magnesium as the larger magnesium ion concentration caused hydroxide ions to be consumed faster. The highest hydroxide ion concentration was found at the outer edge of the femur in the upper right corner of the domain.

4.2 Sensitivity Analysis

For both the pure magnesium and LAE442 implants, sensitivity analysis was performed to investigate the effect of input parameters on the concentrations of magnesium ions, hydroxide ions, and magnesium hydroxide at the point (r = 2.5 mm, z = 240 mm) after 28 days. The input parameters under study were the reaction rate constant, corrosion rate of the LAE442 alloy, hydroxide ion concentration on the outer boundary of the bone, initial concentration of hydroxide ions, and diffusion coefficients of all three species.

The reaction rate constant for the first order reaction of magnesium hydroxide precipitation, which was modeled as a first order reaction, was taken from Zeppenfeld [11]. Due to the large uncertainty in this value, we ran a parametric sweep varying the reaction rate by ± 1 order of magnitude. Since the concentration of hydroxide ions on the outer boundary of the bone was relatively stable, we varied the value used in our model, $2.512 * 10^{-4} mol/m^3$, by only ± 0.2 orders of magnitude. To study the effect of initial concentration of hydroxide in the bone, we ran the model varying the value by ± 2 orders of magnitude.

Because limited literature on magnesium and LAE442 implants was available, we were unable to establish a range of possible diffusivities of magnesium ions, hydroxide ions, and magnesium hydroxide in the bone. The diffusion coefficients of magnesium and hydroxide ions were taken from Oswal, who approximated them as the diffusivities of these species in pure water. The diffusivity of magnesium hydroxide was calculated using Equation 7 (Appendix A). The diffusivity values were varied by ± 1 order of magnitude. Additionally, we varied the corrosion rate of LAE442 by ± 1 order of magnitude. The results of our sensitivity analysis were plotted for the pure magnesium implant and the LAE442 alloy implant (Figures 11-12 respectively).

Figure 11. *Effect of variation in input parameters (a) reaction constant, (b) outer concentration of hydroxide ions, (c) initial concentration of hydroxide ions, (d) diffusivity of magnesium ion, (e) diffusivity of magnesium hydroxide, and (f) diffusivity of hydroxide on output concentrations of magnesium ions, magnesium hydroxide, and hydroxide ions for the pure magnesium implant.*

Variations in the reaction constant affected the output concentration of magnesium hydroxide more than the concentrations of magnesium ions and hydroxide ions (Figure 11). This was expected, given that the concentration of magnesium hydroxide was dependent only on the rate at which it precipitated, k_f. All three species were highly sensitive to variations in the concentration of hydroxide ions at the outer boundary of the bone. Our model was most sensitive to this parameter (Figure 11 b). This indicated that accurate data for this parameter was critical to obtaining a realistic solution.

Our model was less sensitive to variation in initial concentration of hydroxide ions than to changes in the the concentration of hydroxide ions at the outer boundary (Figure 11 c). The concentration of magnesium hydroxide and hydroxide ions were realtively insensitive to variation in the diffusivity of magnesium ions, whereas, the concentration of magnesium ions was sensitive to changes in its own diffusivity (Figure 11 d). Our model was least sensitive to the

diffusivity of magnesium hydroxide; little to no change in the concentration of the three species was observed (Figure 11 e). Finally, our model was highly sensitive to changes in the diffusivity of hydroxide ions (Figure 11 f).

The results of sensitivity analysis for the LAE442 alloy model was also plotted (Figure 12).
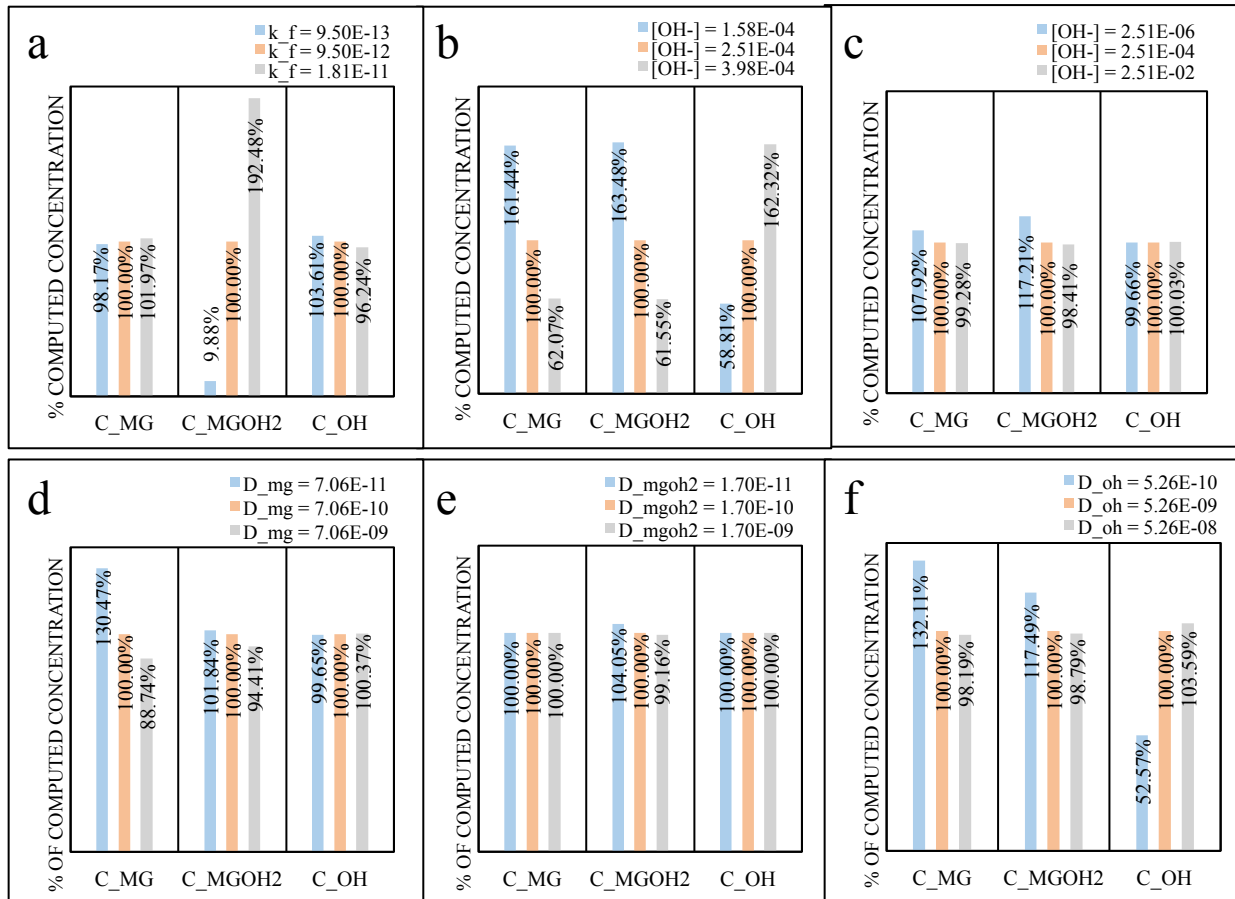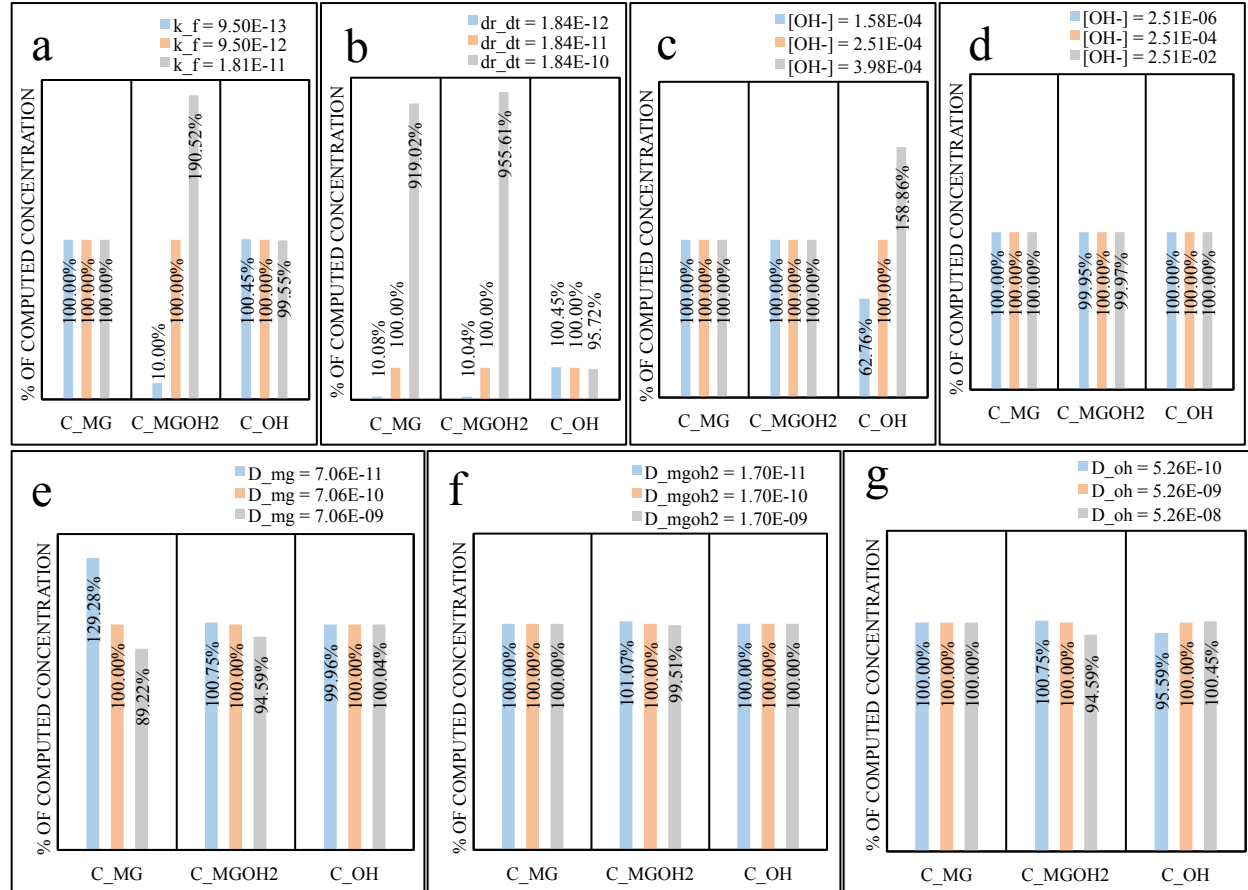

Figure 12. *Effect of variation in input parameters (a) reaction constant, (b) corrosion rate, (c) outer concentration of hydroxide ions, (d) initial concentration of hydroxide ions, (e) diffusivity of magnesium ions, (f) diffusivity of magnesium hydroxide, and (g) diffusivity of hydroxide ions on the concentrations of magnesium ions, magnesium hydroxide, and hydroxide ions for the LAE442 alloy implant.*

Similar to the pure magnesium implant, variations in the reaction constant affected the final concentration of magnesium hydroxide more than the concentrations of magnesium and hydroxide ions (Figure 12). The concentrations of magnesium ions and magnesium hydroxide were more sensitive to variations in the corrosion rate than was the concentration of hydroxide ions (Figure 12 b). The results of this sensitivty analysis indicated that our model of the LAE442 implant was most sensitive to changes in the corrosion rate. Unlike the pure magnesium implant, the corrosion rate of the LAE442 implant was not dependent on pH. Therefore, the output concentrations of the three species were less affected by changes in pH (ie changes in hydroxide ion concentrations) than they were in the pure magnesium model (Figures 12 c and d).

Lastly, the concentration of magnesium ions was more sensitive to changes in the diffusivity of magnesium ions than were the concentrations of magnesium hydroxide and hydroxide ions (Figure 12 e). The output concentrations of the three species showed little to no variation when the diffusivities of magnesium hydroxide and hydroxide ions were changed (Figure 12 f and g).

4.3 Model Validation

In his 2011 study, Oswal modeled the *in vitro* corrosion of both a pure magnesium implant and a magnesium implant with an anodized coating in a 0.15 molar sodium chloride solution after 28 days. While the anodized coating differed from the LAE442 alloy, they were both used as slow-corroding alternatives to pure magnesium implants. The corrosion rate reported by Oswal for the anodized magnesium, 1.05 mm/year, was comparable to that used in our model for the LAE442 alloy, 0.58 mm/year. Therefore, we used data from Oswal on the anodized magnesium to validate our model of the LAE442 alloy. Oswal studied the concentration of magnesium ions, hydroxide ions, and hydrogen gas at steady-state; he did not include the reaction of magnesium ions and hydroxide ions to form magnesium hydroxide. While it would have been ideal to find data from a more similar experiment, such validation was not possible because of the novelty of our model. The corrosion rate as well as magnesium ion and hydroxide ion concentrations obtained by Oswal were compared to those calculated by our model at 28 days (Figure 13).
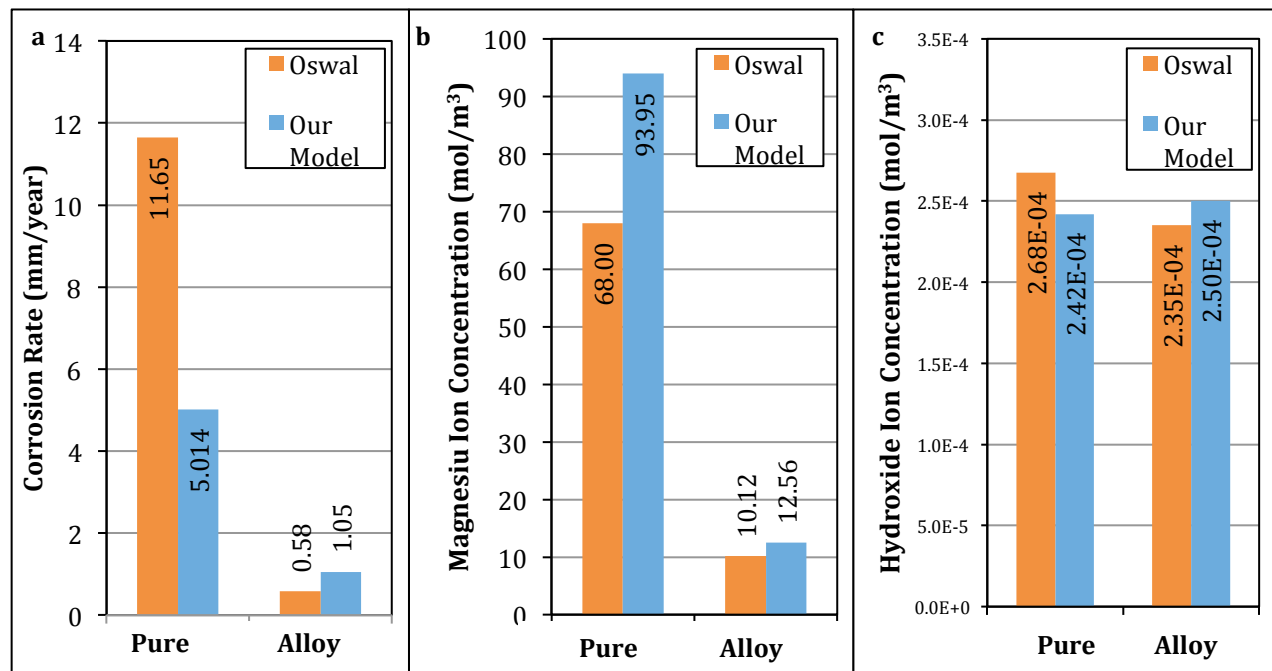

Figure 13. *Comparison of results obtained by Oswal and our model at 28 days.*

As discussed previously, the corrosion rate of the pure magnesium implant was determined by our model, while the corrosion rate of the alloy was taken from *in vivo* data and used as an *input* parameter for the alloy model. The alloy corrosion rate was displayed here because it was similar to that found by Oswal and provided further support for comparing the magnesium and hydroxide ion concentrations produced by the anodized magnesium implant (Oswal) to those produced by the LAE442 implant (our model) (Figure 13 a).

The concentration values shown in Figure 13 b and c were the maximum concentrations of the given species on the implant surface. The magnesium and hydroxide ion concentrations predicted by Oswal's model were on the same order of magnitude as those calculated from our model. The differences between the concentrations determined from the two models were small given the high sensitivity of the concentrations to variations in the input parameters (Section 4.2).

No data currently exists on the concentration of magnesium hydroxide in the bone following implantation of pure or alloyed magnesium. Both Oswal and Yun et al., however, have noted the importance of monitoring and/or modeling the concentration of this species as it precipitated at relatively low concentrations and is potentially toxic in the body [2,7].

5.0 Conclusion

5.1 Design Recommendations and Limitations

The goal of this project was to develop a model of the corrosion of both pure magnesium and the magnesium alloy LAE442 when implanted into the medullary cavity of the femur as a rod. More specifically, we aimed to determine the time required for complete corrosion of the pure magnesium rod in order to compare it to the corrosion rate of the LAE442 implant, which was taken from *in vivo* experimental data. Secondly, we wanted to monitor the concentration profiles of magnesium ions, hydroxide ions, and magnesium hydroxide in order to assess the toxicity of both implant materials.

The corrosion rate of the pure magnesium implant was found to be 5.017 mm/year. This was approximately ten times greater than the corrosion rate of the LAE442 implant, which Witte et al. found to be 0.58 mm/year during *in vivo* experiments [12]. We noted from Figure 3 that the pure magnesium implant degraded completely in 182 days, whereas the LAE442 alloy implant degraded in 1570 days. Our model indicated that the LAE442 alloy implant was more resistant to corrosion than the pure magnesium implant when implanted into the human femur.

Our second objective was to determine the concentration of magnesium ions, hydroxide ions, and magnesium hydroxide in the femur after 28 days. The maximum concentrations of magnesium ions in the femur after 28 days were 93.95 mol/m^3 and 12.56 mol/m^3 for the pure magnesium and LAE442 implants, respectively. Magnesium ions are found throughout the body at high concentrations and play a critical role in many aspects of cellular metabolism. For this reason, the concentration of magnesium ions itself cannot be used to assess the toxicity of magnesium-based implants. Rather, the amount of hydrogen gas evolved, which is directly

proportional to the concentration of magnesium ions evolved from the implant, establishes the toxicity of a given implant.

In a reaction that occurred in parallel to Equation 4, one milliliter of hydrogen gas was evolved for every milligram of magnesium ions produced from the surface of the implant [3]. Song et al. specified the acceptable rate of hydrogen evolution as $9.77*10^{-3}$ mL/day. Taking this to be equivalent to $9.77*10^{-3}$ milligrams of magnesium ions per day, carrying out the proper unit conversions, and multiplying by the duration of the study, 28 days, resulted in a value for the maximum tolerable amount of magnesium that can be produced: $1.13*10^{-5}$ moles. This value was lower than the amount of magnesium ions produced by the corrosion of both the pure magnesium and LAE442 implants, suggesting that use of either implant in humans would not be feasible. Our model indicated that the alloy was *not* a viable alternative for reducing toxicity, stemming from magnesium ions and the corresponding hydrogen gas produced.

This large magnesium ion concentration, however, may be caused by an unrealistic boundary condition on the outer surface of the femur. In an *in vivo* study of magnesium metabolism in sheep, Robson et al. found that there was no appreciable reabsorption of magnesium from the bone into the surrounding tissue [13]. For this reason, a zero-flux boundary condition was applied for magnesium ions on the outer surface of the femur. However, Robson et al.'s study did not involve use of a magnesium implant. Thus, there is no data available on the flux of magnesium ions from the bone when a magnesium implant is present. As these implants introduced unnaturally high concentrations of magnesium ions into the bone, the zero-flux condition taken from Robson et al. may not apply.

In addition to studying the concentration of magnesium ions, we monitored the concentration of hydroxide ions during the corrosion of both implants. The concentration of hydroxide ions was especially important as it affected the pH within the bone. The hydroxide ion concentration changed little from the initial concentration, $2.512*10^{-4}$ mol/m^3 or pH 7.4, in the case of the LAE442 implant. The pure magnesium implant, however, resulted in a decrease in hydroxide ion concentration to a minimum of $2.400*10^{-4}$ mol/m^3 in the femur after 28 days and $2.108*10^{-4}$ mol/m^3 once the implant was fully degraded. This hydroxide ion concentration corresponded to a pH value of 7.38. This is a small pH change that would not cause cell death. Our model indicated that neither the pure magnesium nor the LAE442 alloy produced toxic concentrations of hydroxide ions.

Finally, we monitored the concentration of magnesium hydroxide following implantation of pure magnesium and LAE442. The maximum concentration of magnesium hydroxide in the femur implanted with pure magnesium was $1.074*10^{-3}$ mol/m^3 after 28 days. For the LAE442 implant, the maximum concentration was $1.400*10^{-4}$ mol/m^3. Approximately ten times as much magnesium hydroxide was produced by the pure magnesium implant than by the alloy implant after 28 days. No data on the maximum tolerable concentration of magnesium hydroxide in the bone exists. Oswal, however, indicated that formation of any amount of magnesium hydroxide is of concern. Further studies of magnesium hydroxide metabolism are needed to determine the tolerable concentration of this species.

Using COMSOL, a model of the corrosion of both pure magnesium and LAE442 alloy implanted into the human femur was developed. The corrosion rate of the pure magnesium implant was found to be ten times faster than that of the alloy. While the concentrations of hydroxide ions in the femur resulting from both implants were high enough to prevent formation of a toxic acidic environment, both implants resulted in intolerable hydrogen gas levels, as determined from magnesium ion concentrations. Our model indicated that neither the pure magnesium nor the LAE442 alloy would be safe material for use in the human femur. Further work to develop a slower corroding magnesium alloy is needed.

5.2 Future Work

Additional work is needed both to improve the accuracy of this model and the corrosive resistance of currently available magnesium alloys. Although the implementation of our design problem was realistic, there are still ways in which we could improve the accuracy of our model. One key improvement would be to implement the complete three-dimensional femur geometry. This would allow us to observe any points of especially high or low concentrations that may occur at the ends of the femur due to its irregular geometry. Additionally, rods are traditionally stabilized using pins or screws at the top and bottom of the femur. A model that incorporated the true three dimensional geometry of the femur could also study the effects of these fixation devices.

Further improvements could be made by modeling the different layers of the bone, such as cortical and cancellous bone. The different properties of these layers would affect the diffusivity of each species and, therefore, the final concentration profiles. Furthermore, in our model we focused on three species (magnesium ions, hydroxide ions, and magnesium hydroxide) and modeled the forward reaction noted in Equation 4 (Appendix A). There are many other species and reactions occurring in the body that could potentially affect the corrosion process, such as chloride ion concentration and the reverse reaction by which magnesium hydroxide dissolves into its constituent ions.

As discussed above, the no-flux boundary condition applied on the outer surface of the femur may not be realistic in cases of extremely high magnesium ion concentration as seen with magnesium implants. Further investigation of magnesium metabolism and kinetics *in vivo* is needed to determine if there is any transfer of magnesium ions from the bone following use of magnesium implants. Experimental study of magnesium hydroxide reaction kinetics and the diffusivity of all three species, especially hydroxide ions, would be needed to provide greater certainty to the parameters used in this model. Finally, our model dealt only with erosion corrosion but other types of corrosion, including pitting corrosion and galvanic corrosion, are involved in the degradation of magnesium implants and should be included in future models of this process.

Thus far, we have discussed future work that can be done to improve the accuracy of the current model. However, validation based on data from Oswal indicated that our model produced realistic results at 28 days. Therefore, investigation into slower corroding magnesium alloys would be worthwhile, as our model indicated that neither pure magnesium nor LAE442 were suitable materials for use as orthopedic implants in humans.

There are costs associated with developing a more accurate model as well as developing a slower corroding alloy. In terms of economic feasibility, making improvements to the current model to obtain more accurate results would be more cost effective than conducting experiments to develop a slower corroding alloy. Implementing a model with a three-dimensional femur geometry would definitely be cost effective as three dimensional CAD files of the femur are readily available and this improvement is highly recommended. Other refinements, such as accounting for the properties of the different layers of the bone, would require additional *in vivo* experimentation and are not as economically feasible. While conducting studies to develop slower corroding alloys might be expensive, these studies would be highly valuable to the improvements of biodegradable implants and their effectiveness in repairing bone fractures.

6.0 Appendix A: Mathematical Statement of the Problem

6.1 Governing Equations

We modeled the mass transport of three species over the domain shown in Section 3.1. These three species were magnesium ions (Mg^{2+}), hydroxide ions (OH^-), and magnesium hydroxide ($Mg(OH)_2$).

We assumed the following:
- There was no convection within the bone.
- The femur and implants were represented as perfect cylinders.
- The diffusivity of the three species in the bone were equal to that in water.
- The properties of the different layers of the bone were uniform.
- The implant degraded uniformly, maintaining its cylindrical shape. This assumption was well supported by the data from Kraus et al. shown in Figure 1 b.
- The magnesium ions that occurred naturally in the bone did not participate in magnesium hydroxide precipitation.
- The transport of magnesium ions out of the bone does change in the presence of a magnesium implant.
- The pH values in the tissue surrounding the bone were not changed by the pH changes in the bone.
- Only the forward reaction where magnesium hydroxide was formed was modeled; the reverse reaction was ignored.

For each of these species the governing equations are as follows.

$$\frac{\partial c_{Mg}}{\partial t} = D_{Mg}\left[\frac{1}{r}\frac{\partial}{\partial r}\left(r\frac{\partial c_{Mg}}{\partial r}\right) + \frac{\partial^2 c_{Mg}}{\partial z^2}\right] - k_f c_{Mg} \tag{Eq. 1}$$

$$\frac{\partial c_{OH}}{\partial t} = D_{OH}\left[\frac{1}{r}\frac{\partial}{\partial r}\left(r\frac{\partial c_{OH}}{\partial r}\right) + \frac{\partial^2 c_{OH}}{\partial z^2}\right] - 2k_f c_{Mg} \tag{Eq. 2}$$

$$\frac{\partial c_{Mg(OH)_2}}{\partial t} = D_{Mg(OH)_2}\left[\frac{1}{r}\frac{\partial}{\partial r}\left(r\frac{\partial c_{Mg(OH)_2}}{\partial r}\right) + \frac{\partial^2 c_{Mg(OH)_2}}{\partial z^2}\right] + k_f c_{Mg} \tag{Eq. 3}$$

The erosion corrosion of solid magnesium occurred from the wearing away of the metal surface when immersed in the body. In an aqueous physical environment, solid magnesium readily dissolved into magnesium ions. Magnesium ions reacted with hydroxide ions to form a magnesium hydroxide precipitate, as expressed by the following reaction [2].

$$Mg^{2+} + 2OH^- \rightarrow Mg(OH)_2 \tag{Eq. 4}$$
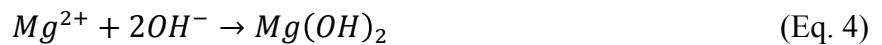
In our model we considered only the forward reaction; we assumed that magnesium hydroxide does not break down into its constituent ions. The forward reaction rate constant, k_f, was taken to be $9.5 *10^{-12}$ (1/s), which was a first order rate constant [11]. The rate of the forward reaction depended only on the concentration of magnesium ions.
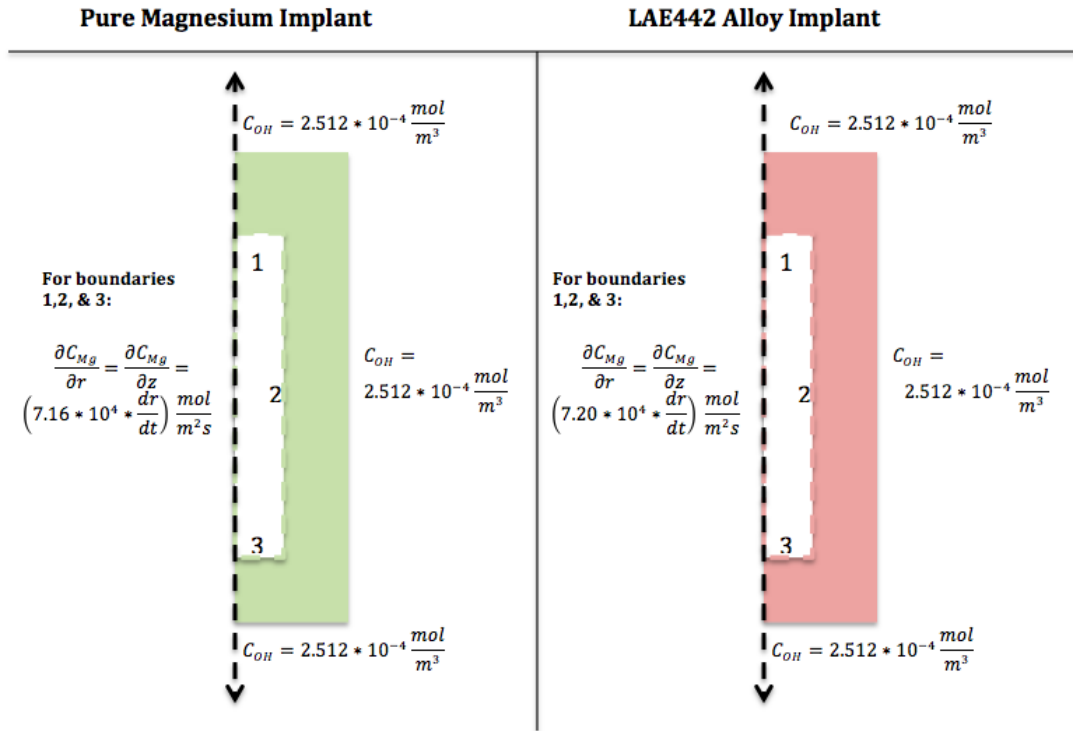
6.2 Boundary and Initial Conditions

Figure 18. *Boundary conditions for the pure magnesium and LAE442 implant.*

Implant-Bone Interface

For the three boundaries between the implant and the bone we specified a flux of magnesium ions for each implant. We assumed that the flux of both hydroxide ions and magnesium hydroxide into the bone from the implant was zero. These species were only evolved or consumed via the above reactions.

As the implant corroded, the boundary between the implant and the bone moved inward toward the axis of symmetry. The velocity of this boundary was different for the pure magnesium and magnesium alloy implants.

In vivo data for the corrosion of the LAE442 alloy was readily available; here we used data from Witte et al. on the corrosion rate of LAE442 implanted into a rabbit femur. They reported a corrosion rate of 0.58 mm/year, or $1.84*10^{-11}$ m/s. This was the constant value that we used for the corrosion rate $\frac{\partial r}{\partial t}$ of the LAE442 alloy. In order to get a flux boundary condition, we multiplied the corrosion rate, $\frac{\partial r}{\partial t}$, by the density of the alloy (Table 2) and divided by the molecular weight of magnesium.

No *in vivo* data for corrosion of pure magnesium implants was available, so we used data from *in vitro* experiments to determine velocity of the moving boundary. These experiments were carried out at a constant pH. However, the pH *in vivo* varies. As demonstrated by Ng et al.,

pH had a large effect on the corrosion rate of magnesium. The following data was used to determine the pH dependence of pure magnesium corrosion [14].

Table 1. pH dependence of pure magnesium corrosion rate

pH	Penetration Rate ($\frac{\partial r}{\partial t}$)	Penetration Rate ($\frac{\partial r}{\partial t}$) in m/s
5.5	$841\ \mu m/day$	$9.73 \times 10^{-9}\ m/s$
6.2	$360\ \mu m/day$	$4.17 \times 10^{-9}\ m/s$
6.8	$125\ \mu m/day$	$1.45 \times 10^{-9}\ m/s$
7.4	$5.92\ \mu m/day$	$6.85 \times 10^{-11}\ m/s$
8.0	$2.93\ \mu m/day$	$3.39 \times 10^{-11}\ m/s$

*The penetration rate was given as the distance normal to the magnesium surface that degraded each day and was highly dependent on pH (Witte, Kaese, et. al).

Fitting an exponential equation to this curve resulted in the following relationship between pH and, $\frac{\partial r}{\partial t}$, the velocity of the moving boundary, with an R^2 value of 0.94.

$$\frac{\partial r}{\partial t} = -0.013 e^{-2.475 \times pH} \qquad \text{(Eq. 5)}$$

The pH included in the above equation depended on the concentration of hydroxide ions present as governed by the following equation:

$$pH = 14 + log_{10}(c_{OH} * 10^{-3}) \qquad \text{(Eq. 6)}$$

Similar to the alloy, we obtained a flux boundary condition by multiplying the corrosion rate, $\frac{\partial r}{\partial t}$, (Equation 5) by the density of the pure magnesium implant (Table 2) and dividing by the molecular weight of magnesium.

Outer Bone Boundaries

At the three remaining boundaries, those between bone and the surrounding environment, the fluxes of magnesium ions and magnesium hydroxide were zero, as there was no appreciable reabsorption of magnesium ions from the bone into the surrounding tissue or circulation [13]. The concentration of hydroxide ions at those boundaries was set to $2.512 * 10^{-4}$ mol/m^3, which was the concentration of hydroxide ions at biological pH. This was obtained using Equation 6 shown above.

Initial Conditions

Initially, the concentration of magnesium hydroxide was zero in the bone. The concentration of hydroxide ions was that normally found at pH 7.4, $2.512 * 10^{-4}$ mol/m^3. The concentration of magnesium ions in the bone was 0 mol/m^3, as we assumed that the magnesium ions naturally found in the bone did not have an effect on the implant reaction.

6.3 Material Properties and Input Parameters

Table 2. Input Parameters

Term		Variable	Value	Source
Diffusion Coefficients	Mg^{2+}	D_{Mg}	$7.063\times10^{-10}\ m^2/s$	Oswal 2011
	OH^-	D_{OH}	$5.260\times10^{-9}\ m^2/s$	Oswal 2011
	$Mg(OH)_2$	$D_{Mg(OH)2}$	$1.70\times10^{-10}\ m^2/s$	Sigma-Aldrich
Density	Femur Bone	ρ_{bone}	$2000\ kg/m^3$	Bensamoun 2004
	Magnesium	ρ_{Mg}	$1.74\times10^6 g/m^3$	Bentor 2012
	LAE442 Alloy	ρ_{LAE442}	$1.75\times10^6 g/m^3$	Witte, et al. 2005
Molecular Weight	Mg	MW_{Mg}	$24.305\ g/mol$	Bentor 2012
Femur Dimensions	Length	l_{femur}	$480\ mm$	Naderi
	Radius	r_{femur}	$11.7\ mm$	Naderi
Implant Dimensions	Length	$l_{implant}$	$400\ mm$	Narang
	Radius	$r_{implant}$	$2.5\ mm$	Narang
Reaction Rate	Rate Constant	k_f	$9.5*10^{-12}\ 1/s$	Zeppenfeld 2011

The diffusivity of magnesium hydroxide was determined using the Einstein-Stokes equation, where k_B was the Boltzmann constant ($1.38*10^{-23}$ m^{2}kg/s^{2}K), T was the temperature (310 K), η was the viscosity of water at body temperature ($6.905*10^{-4}$ kg/m*s), and R was the hydrodynamic radius of magnesium hydroxide [15]. The radius, R, was taken to be $2.9*10^{-9}$ m [16].

$$D_{Mg(OH)_2} = \frac{k_B T}{4\pi\eta R} \qquad \text{(Eq. 7)}$$

Here, we assumed that the fluid properties within the bone were similar to those of pure water. Oswal also made this assumption in his 2011 study, where he determined the diffusivity of magnesium and hydroxide ions through experimentation [2]. All other values were taken directly from the literature (Table 2).

7.0 Appendix B: Solution Strategy

7.1 COMSOL specifications

The direct solver MUMPS, or Multifrontal Massively Parallel sparse direct Solver, was used to solve the algebraic equations associated with the discretization of our model. Time stepping was set to intermediate, ensuring that the solver took at least one time step within each interval specified for storing the solution. For both the pure magnesium and alloy model this time step was 12 hours. The relative tolerance used in the model was 0.01. The default absolute tolerance value of 0.001 was used for magnesium ion concentration but changed to $2.512*10^{-6}$ and $1.1*10^{-5}$ mol/m^3 for hydroxide ions and magnesium hydroxide. This was done to account for the different magnitudes of these concentrations. The final concentration of hydroxide ions at 28 days was approximately $2.512*10^{-4}$ mol/m^3, thus using an absolute tolerance of 0.001 mol/m^3 allowed for too great an error.

7.2 Mesh Convergence

In order to prevent spatial discretization errors and ensure that our results were independent of the mesh, we performed a mesh convergence on our model. This resulted in us choosing a free triangular mesh built with COMSOL's default "extremely fine" settings.
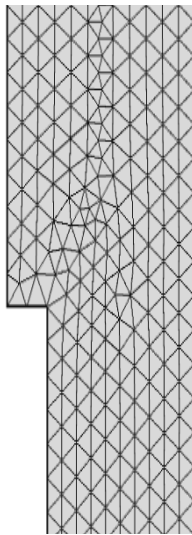

Figure 19. *Final mesh for the pure magnesium implant and the LAE442 alloy implant. The domain contained 24661 elements. Note: only top portion of geometry is shown.*

Mesh convergence analysis allowed us to examine what number of elements was necessary to ensure that our solution did not depend on the mesh. Once this value was reached, the concentrations of magnesium ions, hydroxide ions, and magnesium hydroxide at a given point did not change when a finer mesh was used. Below are the plots for each of the three species after a mesh convergence analysis was performed for both the pure magnesium and LAE442 implants. The point used for mesh convergence was the same as that used in Figures 5, 6, and 7 of the results section (i.e. the point at which the line of planar symmetry intersected the implant-bone interface).
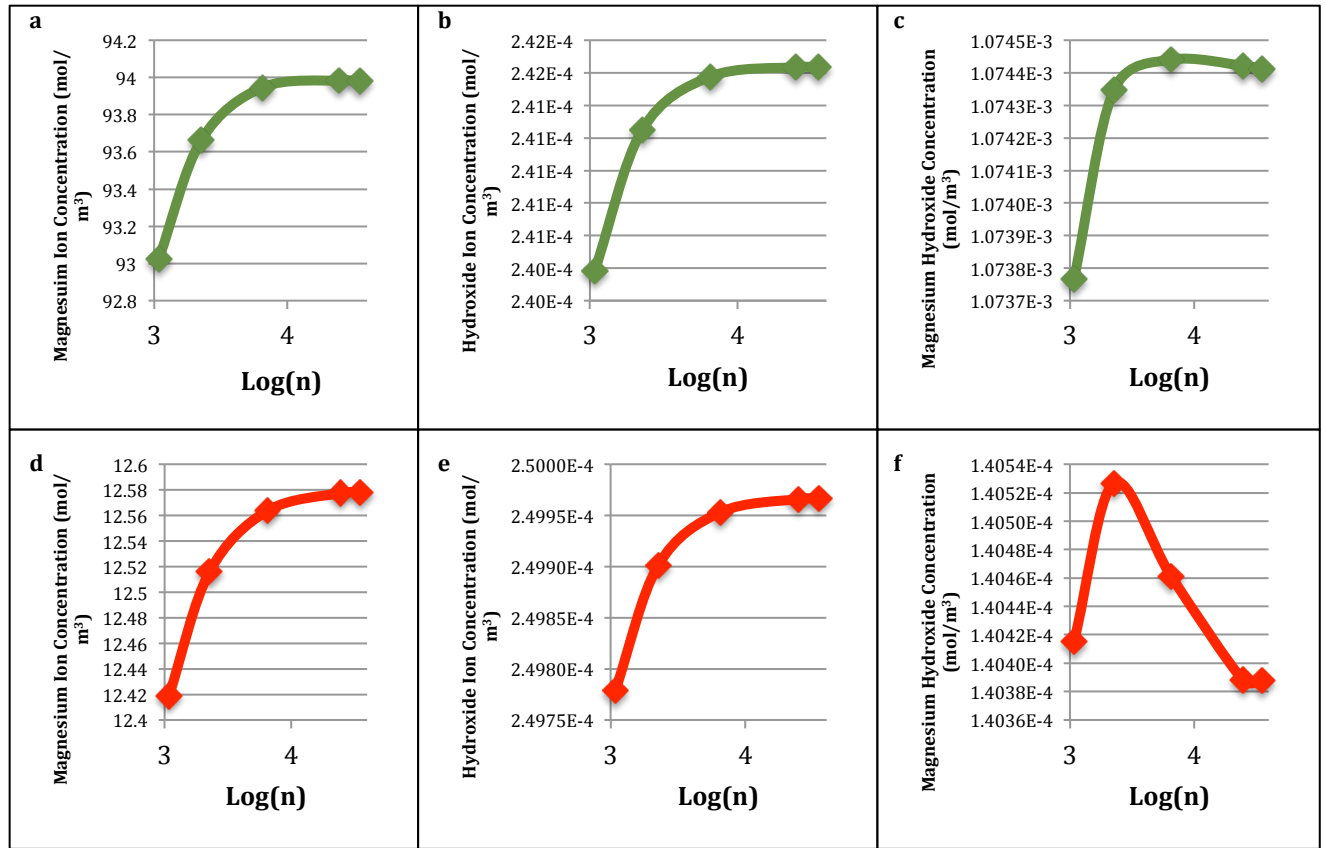
Figure 20. Mesh convergence plots for (a) magnesium ion concentration, (b) hydroxide ion concentration, and (c) magnesium hydroxide concentration in the femur implanted with pure magnesium and (d) magnesium ion concentration, (e) hydroxide ion concentration, and (f) magnesium hydroxide concentration in the femur implanted with LAE442 at the point (r = 2.5 mm, z =240 mm) after 28 days.

7.3 Special Conditions

To prevent the concentrations of magnesium ions and hydroxide ions from becoming negative a step function was implemented as part of the reaction terms for all three species. The reaction term for each of the species was multiplied by the following term: $step1(mod1.c\_mg)$ This step function, step1, gradually changes from 0 to 1 at $1*10^{-9}$. Generally, this step function prevented the reaction from occurring when the concentration of magnesium ions was less than $1*10^{-9}$, or approximately zero.

8.0 Appendix C: References

[1] Broos, P. L. O., & Sermon, A. (2004). From unstable internal fixation to biological osteosynthesis. A historical overview of operative fracture treatment. *Acta chirurgica Belgica*, (4), 396-400.

[2] Oswal, M. (2011). *Analyzing the Corrosion Behavior and Evaluating the Mechanical Integrity of Biodegradable Magnesium Implants* (Doctoral dissertation, University of Cincinnati).

[3] Song, G., & Song, S. (2007). A possible biodegradable magnesium implant material. *Advanced Engineering Materials*, *9*(4), 298-302.

[4] Song, G. (2007). Control of biodegradation of biocompatible magnesium alloys. *Corrosion Science*, *49*(4), 1696-1701.

[5] Samson, E., Marchand, J., & Snyder, K. A. (2003). Calculation of ionic diffusion coefficients on the basis of migration test results. *Materials and Structures*, *36*(3), 156-165.

[6] Witte, F., Kaese, V., Haferkamp, H., Switzer, E., Meyer-Lindenberg, A., Wirth, C. J., & Windhagen, H. (2005). In vivo corrosion of four magnesium alloys and the associated bone response. *Biomaterials*, *26*(17), 3557-3563.

[7] Yun, Y., Dong, Z., Lee, N., Liu, Y., Xue, D., Guo, X. & Fox, C. (2009). Revolutionizing biodegradable metals. *Materials Today*, *12*(10), 22-32.

[8] November 15, 2012. *Fracture and Trauma Treatment in Tampa Bay*. Retrieved from http://chortho.com/specialties/fractures-trauma.php.

[9] Kraus, T., Fischerauer, S. F., Hänzi, A. C., Uggowitzer, P. J., Löffler, J. F., & Weinberg, A. M. (2012). Magnesium alloys for temporary implants in osteosynthesis: in vivo studies of their degradation and interaction with bone. *Acta biomaterialia*, *8*(3), 1230-1238.

[10] Naderi-pour, A. "Femur." *OrthopaedicsOne: The Orthopaedic Knowledge Network*. OrthopaedicsOne, 5 Apr. 2010.

[11] Zeppenfeld, K. (2011). Electrochemical removal of calcium and magnesium ions from aqueous solutions. *Desalination*, *277*(1), 99-105.

[12] Witte, F., et al. "In vivo corrosion and corrosion protection of magnesium alloy LAE442." *Acta Biomaterialia* 6.5 (2010): 1792-1799.

[13] Robson, A. B., Sykes, A. R., McKinnon A. E. and Bell, S. T. (2004). A model of magnesium metabolism in young sheep: transactions between plasma, cerebrospinal fluid and bone. British Journal of Nutrition, 91, pp 73-79.

[14] Ng, W. F., Chiu, K. Y., & Cheng, F. T. (2010). Effect of pH on the *in vitro* corrosion rate of magnesium degradable implant material. *Materials Science and Engineering: C*, *30*(6), 898-903.

[15] "Fluid Viscosity Tables."
http://home.global.co.za/~fluid/GWIS%20Fluid_Viscosity_Table.htm. Feb. 20, 2014.

[16] "Magnesium Hydroxide." *Sigma-Aldrich*. N.p., n.d. Web. 20 Mar. 2014.
<http://www.sigmaaldrich.com/catalog/product/aldrich/632309?lang=en&ion=US>.

[17] S. Bensamoun et al. Journal of Biomechanics 37 (2004) 503–510.

[18] Bentor, Yinon. (2012). "*Chemical Element.com - Magnesium.*" Mar. 27, 2014.

[19] "Kirschner Wire Stainless Steel." *Narang Medical Limited: Orthopaedic Implants & Instruments, India*. N.p., n.d. Web. 5 Mar. 2014.